sciendo
ISSN 1335-8871
MEASUREMENT SCIENCE REVIEW
Journal homepage: https://content.sciendo.com

A Drone as a Reflector Carrier in Laser Tracker Measurements

Michał Jankowski[1], Maciej Sieniło[2], Adam Styk[3]

[1,2]Institute of Metrology and Biomedical Engineering, Faculty of Mechatronics, Warsaw University of Technology, Św. A. Boboli 8, 02-525, Warszawa, Poland, [1]Michal.Jankowski@pw.edu.pl, 2Maciej.Sienilo@pw.edu.pl
[3]The Institute of Micromechanics and Photonics, Faculty of Mechatronics, Warsaw University of Technology, Św. A. Boboli 8, 02-525, Warszawa, Poland, Adam.Styk@pw.edu.pl

Abstract: The paper presents the possibility of mechanizing laser tracker measurements using a drone. Performing measurements using a laser tracker requires touching the measured surface with a probe. Usually it is done manually, even if it requires, e.g., climbing a ladder. The drone was applied as a probe carrier for the laser tracker. To measure a point, the modified drone had to land near this point. Touching the measured surface with the probe was executed using a mobile arm fixed to the drone. This solution allows performing laser tracker measurements without the need of walking or climbing difficult to access surfaces. Two consecutive experiments were performed to verify if such an approach is equally accurate as the standard one (manual measurements). Additionally, the influence of airflow generated by the drones' propellers on a laser wavelength and the accuracy of interferometric measurements were estimated. The research proves that it is possible to mechanize laser tracker measurements using a drone. Moreover, it is demonstrated that the operating drone does not influence the laser tracker accuracy.

Keywords: Laser tracker, laser measurements, interferometric measurement, drone, measurements mechanization.

1. INTRODUCTION

Unmanned aerial vehicles (UAVs), commonly known as drones, are more and more often used in industry in general and specifically in metrology, for example, for large-scale photogrammetry [1]-[4], measurements of antenna radiation patterns [5], gas detection and environmental monitoring [6], and so on. In most of these applications, knowledge of the exact positions of the drone is necessary. These positions can be determined using GPS [3], [6], [7], however, drone GPS accuracy is only in the order of 0.5 - 1 m [8]. This accuracy can be improved to single centimeters by using real-time kinematic positioning (RTK) [4]. In the case of automatic landing, drone position can be determined using several methods, such as observing a set target visible to the drone camera [9], [10] or applying additional sensors, e.g., optical [9]. In this case, the required accuracy is similar to RTK systems. On the other hand, a laser tracker can determine the drone's position more accurately [5]. After fixing a target (a retroreflector) to the drone, the position can be determined with sub-millimeter accuracy. In the case of common contactless measurements, using a drone camera or a drone-mounted LiDAR, laser tracker errors would not be a significant source of measurement errors - possible accuracy is dependent on contactless sensor accuracy. However, it is possible to perform a contact measurement using a drone as a carrier of a laser tracker probe (a retroreflector built into a spherical probe). In this case, the measurement accuracy is dependent only on the accuracy of a given laser tracker.

The setup allowing the measurements using the drone as a probe carrier is shown in Fig.1.

Fig.1. DJI Phantom 3 drone with the prototype landing gear and the mobile arm with the probe.

DOI: 10.2478/msr-2022-0034

The drone was equipped with the landing gear and the attached mobile arm. At the tip of the mobile arm, the probe was fixed. In the measurement procedure, the drone lands near the object to be tested. Further, the landing gear is used to approach the object, and the mobile arm ensures the contact between the probe and the objects' surface.

As stated above, the accuracy of the laser tracker measurements should not depend on the drone positioning accuracy. However, the accuracy of the laser tracker itself depends on multiple factors, such as a gradient of the temperature of the air, vibrations, stability of the probe during measurement, etc. A drone with running motors and rotating propellers may significantly influence these factors. For example, let us consider the influence of the air movement forced by drone propellers. According to Bernoulli's principle, air movement causes a decrease in the moving air's pressure. Therefore, it causes measurement error as air pressure, according to Edlén's and Ciddor's equations [11]-[14], is one of the most important factors influencing a refractive index of air. Consequently, the refractive index gradient is one of the significant sources of measurement errors in the laser tracker measurements, as light wavelength, a gauge in all interferometric measurements, depends on the refractive index.

In conventional measurements using a laser tracker, to measure location of the point, an operator has to touch the measured surface with the probe. Location and dimensions of a measured element are calculated, fitting a geometrical element (e.g., a sphere) to the measured points. Such measurements are accurate, but if the measured element is in a difficult to access location, there is a need to move the operator near this location. This problem can be overcome by using a drone to transport the probe to the desired location. However, it was unclear if using a drone instead of an operator's hand would worsen the uncertainty of the measurement.

In this paper, the research of this problem is presented. The authors compare laser tracker measurement results in two cases: 1) conventional operation of the laser tracker, with the probe carried by an operator, and 2) drone-assisted measurements in which the drone carried the probe. In this case the probe was fixed to the end of a mechanized arm which was fixed to the drone. To measure a point, the drone had to land near this point. Then the mechanized arm moved the probe, so it finally touched the measured surface. Because of the technical reasons described in section 2, the drone motors were kept running. That is why the obtained results can be generalized and, e.g., applied in situations in which a flying drone position is determined using a laser tracker like in [5].

In the second section of the paper, measured objects and measurement tasks are presented. In the third section, the statistical analysis of the results is described. Finally, the conclusions are drawn.

2. SUBJECT & METHODS

Drones use various sensors for navigation. Usually, one of them is a magnetometer, used as a compass. Since it is a delicate instrument, large steel objects or magnets may interfere with its operation. That is why in the case of the DJI Phantom 3 Advanced drone used in this research, it must be switched on far away from heavy steel objects or strong magnets. If this condition is not met, the drone will not switch the motors on. That is why it was assumed that even after landing, motors should keep running, and propellers should keep rotating. In consequence, laser tracker measurements using the drone as the probe carrier are influenced by the movement of the air. This movement changes the air pressure, which affects the air refractive index. If v is the speed in m/s and ρ is the density of the air in kg/m^3, the change of the pressure of the air Δp in Pa can be determined using Bernoulli's principle (1).

$$\Delta p = \frac{v^2 \rho}{2} \tag{1}$$

In most cases, the laser tracker uses a weather station to measure the air's temperature, pressure, and humidity. An exact wavelength of the tracker light source may be calculated by knowing these values. However, the weather station is placed in a specific position while the probe is being moved. If the probe is connected with a drone, the drone is the source of a local change of the air refractive index. Because of its locality, this change cannot be determined using the abovementioned weather station.

The wind speed in drone proximity was measured using the anemometer to estimate the influence of not switching off the motors. In the drone vicinity, the measured wind speed was 1.6 m/s, while 75 cm away from the drone – 0.5 m/s. Let us assume that air density, in temperature of 20°C, is equal to 1.204 kg/m^3. If so, the wind speed of 1.6 m/s means Δp equivalent to 1.54 Pa. According to the modified Edlén equation (the online calculator from NIST "Engineering Metrology Toolbox" [15] was used), such change of the air pressure corresponds to He-Ne laser light wavelength change of $2*10^{-6}$ nm. Such changes are negligible - error caused by the calculated difference even at a distance of 750 mm is equal to about 2.4 nm. This means that laser tracker accuracy should not be influenced by the drone propellers operation.

During the experiments, the Leica AT901 laser tracker with a 12.7 mm probe was used. The used tracker can work in two modes: in an interferometer mode, the distance from the base station to the probe is measured using a simple laser interferometer. The interferometer is very accurate, but requires constant line of sight to the probe. In an absolute measurement mode, the distance is measured using a laser rangefinder which enables absolute measurements. This solution enables measurements after breaking the laser beam. Because in measurements of difficult to access surfaces laser beam is frequently broken, all the tests were performed using the absolute mode. However, the sensitivity to environmental factors of the laser rangefinder is similar to that of the laser interferometer.

However, a drone with motors switched on is also a source of vibrations. Additionally, the force between the laser tracker probe and the measured surface is different in the case of manual measurement and drone-aided measurement. Because of these reasons, the authors decided to experimentally determine the influence of the probe-carrying drone on laser tracker accuracy.

Because the measurement uncertainty component caused by the drone operation was investigated, it was decided to measure relatively small artifacts since the measurement uncertainty component dependent on the accuracy of the laser tracker itself is smallest for small and close to the tracker objects. In contrast, expected errors caused by the drone operation should not be dependent on the artifact size, because the air pressure gradient caused by a drone is local and vibrations of a drone are the same at every point of a laser tracker measurement zone.

In the first experiment, an artifact made of two reference spheres, shown in Fig.2., was used, and the distance between the centers of the two spheres was measured. Both spheres have a nominal diameter equal to 25 mm and are made of ceramic. Their locations were determined by the measurement of 5 points on the surface of each of the spheres. The calculations of the spheres' centers were done by the PC-DMIS software. The distance between the centers of the spheres was measured ten times using a drone as a probe carrier and ten times manually. In case of the drone-aided measurements, the drone took off and landed after every measurement of a single sphere from 5 points. The measurement scheme is shown in Fig.3. Distances measured using a drone are signed as LB1 and distances measured manually are signed as LB2.

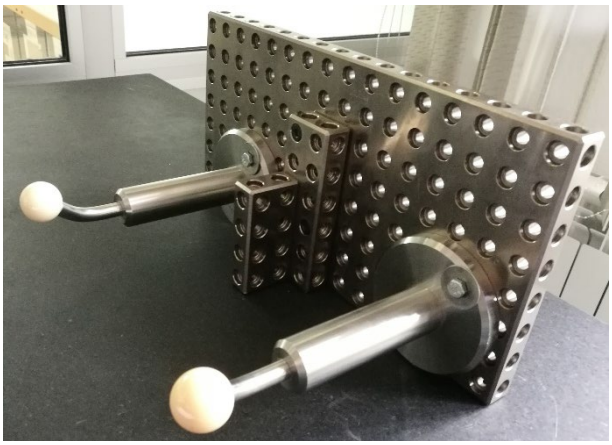

Fig.2. Examined element with ceramic reference spheres of diameter 25 mm.

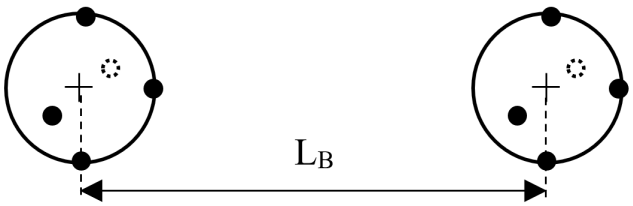

Fig.3. Measuring the distance between the center of the spheres.

In Fig.3., desired positions of measurement points on the spheres are marked. In reality, positions of measurement points varied - it is not possible to take the same point, neither manually, nor using a manually controlled drone as a probe carrier. In the case of measurements performed using a drone, the mobile arm shown in Fig.1. reduced accessible parts of surfaces of the balls. Although the mobile arm can be easily reconfigured, its configuration was not changed during the experiment.

The examined element was fixed to the steel scribing plate using multiple magnetic prisms.

In the second experiment, repeatability in one dimension was determined for manual measurements and drone-aided measurements. The measurement scheme is shown in Fig.4.

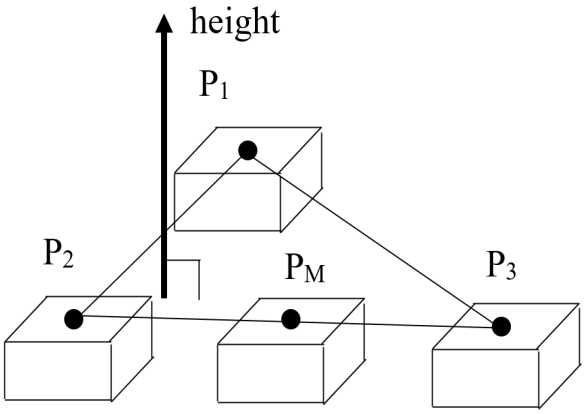

Fig.4. The measurement scheme for the second experiment: P_1, P_2, P_3 - points used to determine the plane and direction, P_M - a point the height of which was measured.

The measurement direction was chosen as perpendicular to the plane defined by central points on surfaces of 3 gauge blocks. The gauge blocks were fixed to the steel scribing plate. The plane was measured only once manually. Then the height (location in the direction perpendicular to the plane) of the top of one gauge block was measured ten times using the drone as a probe carrier and ten times manually. In the case of the drone-aided measurements, the drone took off and landed after every single point measurement.

3. RESULTS

The distance LB measured using the drone (LB1) and manual approach (LB2) is presented in Table 1.

Table 1. The results of L_B distance measurement using the drone (L_{B1}) and manual approach (L_{B2}).

Measurement number	L_{B1} [mm]	L_{B2} [mm]
1	196.776	196.760
2	196.718	196.748
3	196.783	196.771
4	196.808	196.766
5	196.778	196.727
6	196.722	196.735
7	196.720	196.708
8	196.753	196.751
9	196.740	196.742
10	196.741	196.710
Average [mm]	196.753	196.741
Std. deviation [µm]	29	21
Variance [µm^2]	864	433
Range [µm]	90	63

The difference in average distance measured using those two approaches is 12.1 µm. The standard deviation of the drone and manual results is 29.4 µm and 20.8 µm, respectively, and the variance is 864.4 µm^2 and 432.6 µm^2. The value of the range is around 50 % larger in the case of the drone measurement and is equal to 90 µm, whereas, in the case of manual measurement, it is 63 µm.

In the next step, the authors verified if there were any outliers. The StatGraphics software was used for data analysis. Box and Whisker plots of L_{B1} and L_{B2} are presented in Fig.5. Presented Box and Whisker plots show no outliers among the measurement results.

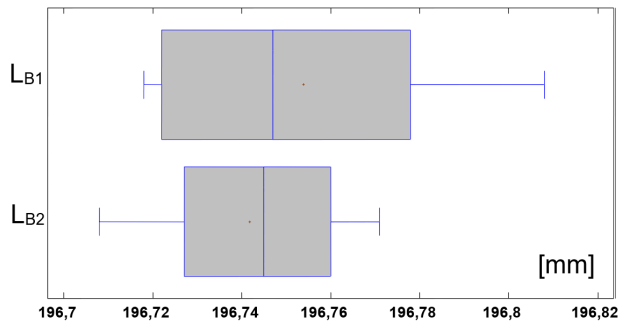

Fig.5. Box and Whisker plots of LB1 and L_{B2}.

The measurement results of the L_P height of the P_M points, located on the top of the gauge block, are presented in Table 2. Height values measured using the drone are described as $L_{P1,}$ and height values measured manually are described as L_{P2}. The difference between the average values of the measured height using the drone and manually is -11 µm. The standard deviation of results obtained using the drone is 11 µm and measured manually is 13 µm. The variance is 128 µm^2 and 144 µm^2, respectively. The value of the range is equal to 33 µm for both the drone and manual measurements. In conclusion, the difference between the L_{P1} and L_{P2} results is minimal.

Table 2. The results of distance measurements between measured point and the direction-defining plane L_P for the drone (L_{P1}) and manual measurement (L_{P2}).

Measurement number	LP1 [mm]	LP2 [mm]
1	0.000	0.026
2	0.019	0.022
3	-0.014	-0.004
4	0.015	0.017
5	0.008	0.019
6	-0.011	0.025
7	0.001	0.020
8	0.010	-0.007
9	-0.014	-0.003
10	0.008	0.013
Average [mm]	0.002	0.013
Std. deviation [µm]	11	12
Variance [µm^2]	128	144
Range [µm]	33	33

Box and Whisker plots (see Fig.6.) also show no outliers among the measurement results.

To confirm this conclusion, Grabbs' test was used. However, before the Grabbs test, the results' normal distribution was to be confirmed. For that purpose, three tests using StatGraphics software were performed. These tests were: Chi-Square, Shapiro-Wilk W, and Skewness Z-score. Their results are shown in Table 3.

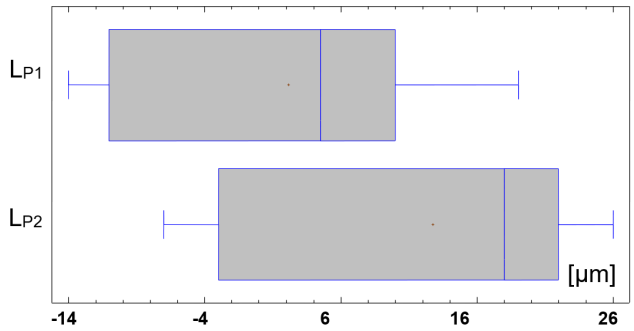

Fig.6. Box and Whisker plot of L_{P1} and L_{P2}.

All tests except one show that the measuring results come from the normal distribution. The p-value for the Shapiro-Wilk test for L_{P2} is lower than 0.05, and so we can reject the hypothesis with 95 % confidence that the results come from a normal distribution. But as the remaining tests indicate that the L_{P2} results come from a normal distribution, it was assumed that the difference between the 0.05 and the obtained p-value is negligibly small.

Table 3. Results of tests for distribution normality for L_{B1}, L_{B2}, $L_{P1,}$ and L_{P2}.

Test	p-value			
	L_{B1}	L_{B2}	L_{P1}	L_{P2}
Chi-Square	0.189	0.780	0.540	0.333
Shapiro-Wilk	0.359	0.615	0.325	0.044
Skewness Z-score	0.673	0.691	0.786	0.433

Using the Grabbs test, the null hypothesis that there are no outliers was tested against the alternative hypothesis that there are outliers. P-value for L_{B1} is 0.595, for L_{B2} is 1.0, for L_{P1} is 1.0 and for L_{P2} is 0.994. Since Grabbs' test's p-value is greater than 0.05, the most extreme values are not a significant outlier at the 5.0 % significance level.

The main goal of calculations was to check if the measurement using the drone is significantly different compared to results measured manually. It was checked both for the results of the 3D distance measurements (L_B, the distance between 2 calibration spheres) and for the 1D location measurements (L_P, the height of the point).

Therefore, in the next step, standard deviations of the two samples ∂_{LB1} and ∂_{LB2}were compared using F-test, the standard deviations of the two samples ∂_{LB1} and ∂_{LB2}. The following hypotheses were made:

$$H_0: \partial_{LB1} = \partial_{LB2}$$

$$H_A: \partial_{LB1} \neq \partial_{LB2}$$

The null hypothesis H_0 must be rejected as the calculated p-value is 0.314. There is no statistically significant difference between the standard deviations of the two samples at the 95.0 % confidence level.

Assuming equal standard deviation, the two-sample comparison test was used. The means of the measured distance $\bar{L}_{B1}$ and $\bar{L}_{B2}$ were investigated. The following hypotheses were made:

$$H_0: \bar{L}_{B1} - \bar{L}_{B2} = 0$$

$$H_A: \bar{L}_{B1} - \bar{L}_{B2} \neq 0$$

To compare the means of the two sets of samples, t-test was used. The obtained p-value is 0.326, so it exceeds 0.05, thus there is no statistically significant difference between the means of the two sets of samples at the 95.0 % confidence level.

The same procedure was used to compare standard deviations ∂_{LP1} and ∂_{LP2} of measurement results for the location (height) of the point. The following hypotheses were made:

$$H_0: \partial_{LP1} = \partial_{LP2}$$

$$H_A: \partial_{LP1} \neq \partial_{LP2}$$

The obtained p-value for the F-test is 0.863, so there is also no statistically significant difference between the standard deviations of the two samples L_{P1} and L_{P2} at the 95.0 % confidence level.

As a consecutive step, the means $\bar{L}_{P1}$ and $\bar{L}_{P2}$ were compared using the F-test under the assumption of equal standard deviations. The following hypotheses were made:

$$H_0: \bar{L}_{P1} - \bar{L}_{P2} = 0$$

$$H_A: \bar{L}_{P1} - \bar{L}_{P2} \neq 0$$

The p-value of t-test is 0.069, so there is no statistically significant difference between the means of the two samples at the 95.0 % confidence level.

Due to the lack of confirmation of the normal distribution of L_{P2} results with the Shapiro-Wilk test, it was decided to verify this using the non-parametric Kruskal-Wallis test. This test allows checking an influence of one factor even if the sample does not come from the normal distribution. This analysis verified whether taking measurements using a drone or manually was statistically significant. The Kruskal-Wallis test verifies the null hypothesis that the medians of L_P within each of the two levels of the factor are the same.

The p-value is 0.0536 and is greater than 0.05, so there is no statistically significant difference amongst the medians at the 95.0 % confidence level.

The non-parametric Kruskal-Wallis test confirmed the previous observations that from a statistical point of view, the use of a drone both to measure the distance between the centers of the spheres and to measure the location (height) of the point did not have a significant impact on the measurement results.

4. CONCLUSION

Experiments carried out to determine if the drone can be used as a probe carrier for a laser tracker showed that using a drone does not reduce the accuracy of the measurement. They proved that measured values (3D distance and 1D location) had no statistically significant differences, either for the means or the variations of the results.

The experiments were performed with relatively small artifacts to be able to detect even small additional errors brought in by the use of the drone. However, laser trackers are typically used to measure larger objects, access to which may be limited, e.g., because of the altitude at which they are located. The authors met such a problem while measuring unique positions of reference targets in the separated field-of-views for multi-camera 3D DIC (Digital Image Correlation) system applied to wind turbine blade investigations. Fig.7. presents the photograph of the measurement site of the wind turbine blade (WTB) and the location of the laser tracker. As the WTB is mounted in the test rig 3 m above the ground, the access to the targets measured with the laser tracker was significantly impeded. In such cases carrying a probe by a drone could make measurement faster or safer, for example, eliminating the need to climb using a ladder.

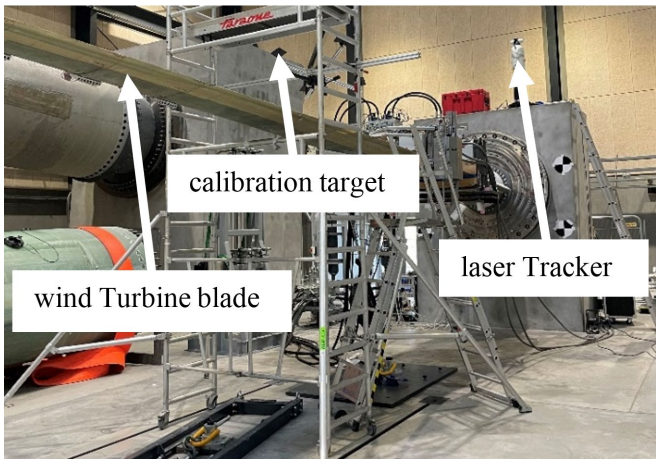

Fig.7. The photograph of the measurement site of the wind turbine blade using the laser tracker.

Moreover, laser trackers are currently used to measure the position of a flying drone. The results presented above suggest that such measurements are equally accurate as standard laser tracker measurements. Although flying the drone generates unwanted airflow, the associated air pressure change should still be negligible.

A lack of information if the probe touched the measured surface caused the main problem during the drone-aided measurements. During the presented experiments, it was assessed by the drone operator. Because such assessments are challenging and need some experience, it would be beneficial to detect the contact automatically, e.g., using a strain gauge. The signal from the strain transducer could switch on a LED or even directly trigger laser tracker readout.

Another direction of further research and possible development of the described system is to eliminate the need to land before every measurement. At this moment, the drone

has to land near or on the measured object. However, it might be possible to touch a measured object with a probe and take measurement points without landing.

There is also the possibility of developing a lighter system using a smaller drone that would be safer.

ACKNOWLEDGMENT

This work was sponsored by statutory funds [institution: Warsaw University of Technology, Scientific Council of the Discipline of Mechanical Engineering].

The authors would like to thank Mr. Ignacy Jackl for assistance in the landing gear construction, M.Sc. Eng. Andrzej Jankowski for assistance in the drone operations and M.Sc. Eng. Alex Stelmach for lending the anemometer.

REFERENCES

[1] Tournadre, V., Beilin, J., Pierrot-Deseilligny, M., Faure, P.-H. (2016). Accurate 3D models for a 4D monitoring of linear hydraulic structures: Opportunities and characteristics of UAV. *La Houille Blanche*, 102 (3), 33-38. https://doi.org/10.1051/lhb/2016028

[2] Tournadre, V., Pierrot-Deseilligny, M., Faure, P.H. (2015). UAV linear photogrammetry. *The International Archives of the Photogrammetry, Remote Sensing and Spatial Information Sciences*, XL-3/W3, 327-333. https://doi.org/10.5194/isprsarchives-XL-3-W3-327-2015

[3] Rutkiewicz, J., Malesa, M., Karaszewski, M., Forys, P., Siekanski, P., Sitnik, R. (2018). The method of acquiring and processing 3D data from drones. In *Speckle 2018: VII International Conference on Speckle Metrology*. SPIE 10834, 558-564. https://doi.org/10.1117/12.2319717

[4] Menna, F., Nocerino, E., Remondino, F., Saladino, L., Berri, L. (2020). Towards online UAS-based photogrammetric measurements for 3D metrology inspection. *The Photogrammetric Record*, 35, 467-486. https://doi.org/https://doi.org/10.1111/phor.12338

[5] Fritzel, T., Steiner, H.-J., Strauß, R. (2018). Laser tracker metrology for UAV-based antenna measurements. In *2018 IEEE Conference on Antenna Measurements Applications (CAMA)*. IEEE, 1-3. https://doi.org/10.1109/CAMA.2018.8530613

[6] Daponte, P., De Vito, L., Mazzilli, G., Picariello, F., Rapuano, S., Riccio, M. (2015). Metrology for drone and drone for metrology: Measurement systems on small civilian drones. In *2015 IEEE Metrology for Aerospace (MetroAeroSpace)*. IEEE, 306-311. https://doi.org/10.1109/MetroAeroSpace.2015.7180673

[7] Brzozowski, B., Rochala, Z., Wojtowicz, K. (2017). Overview of the research on state-of-the-art measurement sensors for UAV navigation. In *2017 IEEE International Workshop on Metrology for AeroSpace (MetroAeroSpace)*. IEEE, 565-570. https://doi.org/10.1109/MetroAeroSpace.2017.7999532

[8] Tahar, K.N., Kamarudin, S. (2016). UAV onboard GPS in positioning determination. *The International Archives of the Photogrammetry, Remote Sensing and Spatial Information Sciences*, XLI-B1, 1037-1042. https://doi.org/10.5194/isprs-archives-XLI-B1-1037-2016

[9] Borovytsky, V., Averin, D. (2020). Optical sensor for drone coordinate measurements. In *Optics and Photonics for Advanced Dimensional Metrology*. SPIE 11352, 324-329. https://doi.org/10.1117/12.2555392

[10] Cocchioni, F., Mancini, A., Longhi, S. (2014). Autonomous navigation, landing and recharge of a quadrotor using artificial vision. In *2014 International Conference on Unmanned Aircraft Systems (ICUAS)*. IEEE, 418-429. https://doi.org/10.1109/ICUAS.2014.6842282

[11] Ciddor, P.E. (1996). Refractive index of air: New equations for the visible and near infrared. *Applied Optics*, 35, 1566-1573. https://doi.org/10.1364/AO.35.001566

[12] Birch, K.P., Downs, M.J. (1994). Correction to the updated Edlén equation for the refractive index of air. *Metrologia*, 31, 315-316. https://doi.org/10.1088/0026-1394/31/4/006

[13] Birch, K.P., Downs, M.J. (1993). An updated Edlén equation for the refractive index of air. *Metrologia*, 30, 155-162. https://doi.org/10.1088/0026-1394/30/3/004

[14] Edlén, B. (1966). The refractive index of air. *Metrologia*, 2, 71-80. https://doi.org/10.1088/0026-1394/2/2/002

[15] NIST. *Engineering Metrology Toolbox - Refractive index of air calculator based on modified Edlén equation. [Online calculator]*. https://emtoolbox.nist.gov/Wavelength/Edlen.asp

Received January 12, 2022
Accepted July 22, 2022